2016

Numerical Simulation of the 3d Transient Temperature Evolution Inside a Domestic Single Zone Wine Storage Cabinet With Forced Air Circulation

Johann Hopfgartner
TU Graz, Austria, hopfgartner@ivt.tugraz.at

Martin Heimel
TU Graz, Austria, heimel@ivt.tugraz.at

Stefan Posch
TU Graz, Austria, posch@ivt.tugraz.at

Erwin Berger
TU Graz, Austria, berger@ivt.tugraz.at

Raimund Almbauer
TU Graz, Austria, almbauer@ivt.tugraz.at

See next page for additional authors

Numerical Simulation of the 3d Transient Temperature Evolution Inside a Domestic Single Zone Wine Storage Cabinet with Forced Air Circulation

Johann HOPFGARTNER[1]*, Martin HEIMEL[1], Erwin BERGER[1], Stefan POSCH[1], Raimund ALMBAUER[1], Stephan SCHLEMMER[2]

[1]Institute of Internal Combustion Engines and Thermodynamics, Graz University of Technology, Inffeldgasse 19, 8010 Graz, Austria

hopfgartner@ivt.tugraz.at, +43 316 873 30240
heimel@ivt.tugraz.at, +43 316 873 30235
berger@ivt.tugraz.at, +43 316 873 30234
posch@ivt.tugraz.at, +43 316 873 30233
almbauer@ivt.tugraz.at, +43 316 873 30230

[2]Liebherr-Hausgeraete Lienz GmbH, Dr.-Hans-Liebherr-Strasse 1, 9900 Lienz, Austria

stephan.schlemmer@liebherr.com, +43 50809 21310

* Corresponding Author

ABSTRACT

This work is carried out in order to investigate the air flow and temperature stratification in the compartment of a single zone wine storage cabinet with forced ventilation for domestic use. The appliance used in this work has a total gross capacity of approximately 135 liters. A single zone wine cooler should achieve evenly distributed temperature for all bottles inside the appliance. To analyze the temperature distribution, a numerical simulation of the air flow and the temperature field can be very helpful.

The numerical simulations are carried out applying commercial CFD (Computational Fluid Dynamic) software using the finite volume method. Therefore, the following assumptions are made: the evaporator is modelled by means of a time-varying but locally constant temperature obtained from measurements, the ambient temperature is constant. Concerning the air flow, turbulent conditions are considered. The energy equation is solved transiently and the flow field is calculated assuming steady-state conditions at specific points in time in order to reduce computing time. Furthermore, the air flow in the air channel behind the rear and the top wall of the compartment, where the fan and the freely suspended evaporator are located, is also simulated. The compartment is investigated for different configurations: firstly, an empty wine cooler only with wooden grid shelves and secondly, an appliance loaded with test packages. Temperature measurements with several thermocouples inside the compartment and the air channel are carried out for each arrangement to verify the results of the numerical simulations.

1. INTRODUCTION

Approximately one fourth of the electrical energy spend in a typical European household is used for refrigeration applications including freezers and refrigerators (De Almeida *et al.*, 2011). Thereby, a decreasing trend of the specific energy consumption of these appliances can be observed due to the distribution of new appliances with higher efficiencies driven by labelling and eco-design regulations (Bosseboeuf, 2015). Further efficiency improvements will probably only be possible by a combination of experiments and numerical simulation tools such as CFD. One field of application for CFD simulations is the investigation of the thermal evolution and the air flow inside the compartments of refrigeration appliances. Apart from high efficiency, an evenly distributed temperature inside every temperature zone, or inside the whole compartment for single zone appliances, is one of the major goals within the development process of refrigerators. This also applies to wine storage cabinets.

Several studies have been carried out in the field of domestic refrigeration, especially the temperature and air flow distribution in compartments were subject of investigations. Hermes *et al.* (2002) presented a CFD code for the 2d buoyancy driven flow inside a refrigerated cabinet using the Boussinesq approximation. Thereby, an incompressible laminar flow was assumed. Other studies of the flow field due to natural convection in domestic refrigerator applications were done by Bayer *et al.* (2013), Ben Amara *et al.* (2008) and Laguerre *et al.* (2007). Ben Amara *et al.* (2008) investigated the flow field in a domestic refrigerator in order to determine the thickness of the hydrodynamic boundary layers. They compared PIV (particle image velocimetry) measurements with numerical simulations assuming laminar 3d flows taking radiation effects into account. Laguerre *et al.* (2007) studied the heat transfer by natural convection in a domestic refrigerator without ventilation. The numerical simulation was done by using commercial CFD software supposing a 3d laminar air flow. The authors compared simulations considering and neglecting radiation heat transfer with measurements and came to the result that the neglect of the radiation leads to more pronounced temperature stratifications. Bayer *et al.* (2013) simulated the fluid flow and temperature distribution, assuming a three-dimensional, turbulent and transient flow problem. Their results do not show a significant change of the temperature distribution inside the refrigerator when considering heat transfer by radiation, however, heat rates are affected drastically. These examples indicate that in relevant publications on the subject of air flow in refrigerators without ventilation, mostly laminar flow conditions are assumed and thermal radiation should be taken into account. There are also several studies concerning the air flow in refrigerators with forced ventilation. Lee *et al.* (1999) studied the air flow characteristics in a refrigerator with forced air circulation using PIV and numerical simulations. The results of the simulation supposing a turbulent, 3d and steady-state flow, showed good agreement with the PIV measurements. Further investigations of the thermal uniformity inside refrigerator appliances with forced ventilation were carried out by Belman-Flores *et al.* (2013), Fukuyo *et al.* (2003) and Yang *et al.* (2010). They all assumed turbulent and three-dimensional flow conditions and did not consider thermal radiation effects.

All these examples of different studies show that the topic around the thermal stratification inside the compartment of a refrigerator is still important and simulations can be very extensive. Due to the high numerical effort, especially for calculating the temperature evolution during a longer period of time, the current paper uses an approach where the computing time is reduced by decoupling the calculation of the energy equation and the flow field. This means, that the energy equation is solved completely transiently whereas the equations of momentum and continuity are only solved at specific points in time. During the transient calculation of the energy equation, steady-state conditions for the flow field are assumed. Thereby, radiation effects are not considered and a turbulent flow regime is supposed. The investigated refrigerator is a single zone wine storage cabinet with forced convection. Two different loading conditions of the compartment are investigated: empty cooling device only with its wooden grid shelves and loaded with three test packages. A comparison between simulated and measured data shows moderate deviations in temperature which result mainly from the simplified temperature profile of the evaporator and the coarse approximation of the solid parts.

2. EXPERIMENTAL SETUP

The investigated refrigerator is a single zone wine storage cabinet with a total gross capacity of approximately 135 liters. The cabinet is equipped with three wooden grid shelves which enable the storage of at most 46 bottles (á 0.75 liters). Inside the compartment, the temperature can be regulated in a range of +5 °C to +20 °C and heat transfer is mainly done by forced convection generated by a fan with two operating modes. Either, the fan is only running when the compressor is also switched on, or it is running permanently at two different rotational speeds depending on the compressor's state. In this work, the thermostat inside the compartment is set to +12 °C and the permanent mode of the fan is enabled. Figure 1 shows two cross sections of the wine storage cabinet being loaded with test packages (TP1-TP3), in which the temperature measuring positions are indicated. The warm air inside the compartment is sucked through an air grille by the axial fan and passed via an air duct to the freely suspended evaporator. There, the air is cooled down and discharged at the ventilation slot at the backside of the compartment. To validate the simulation results, three temperature measurement points along the air duct and nine inside the compartment are used. Table 1 shows the distances named "a" to "i" which can be seen in Figure 1. The used T-type thermocouples with an accuracy ±0.5 K are fixed on small copper plates with a thermal capacity of approximately 0.16 J/K. These copper plates facilitate the mounting and damp the noisy fluctuations of the temperature. The lower picture on the right side of Figure 2 shows a close-up view of such a thermocouple. On the remaining pictures of Figure 2, the experimental arrangement within the compartment and the three measurement points mounted on the evaporator can be seen on the left side and on the top right side, respectively.

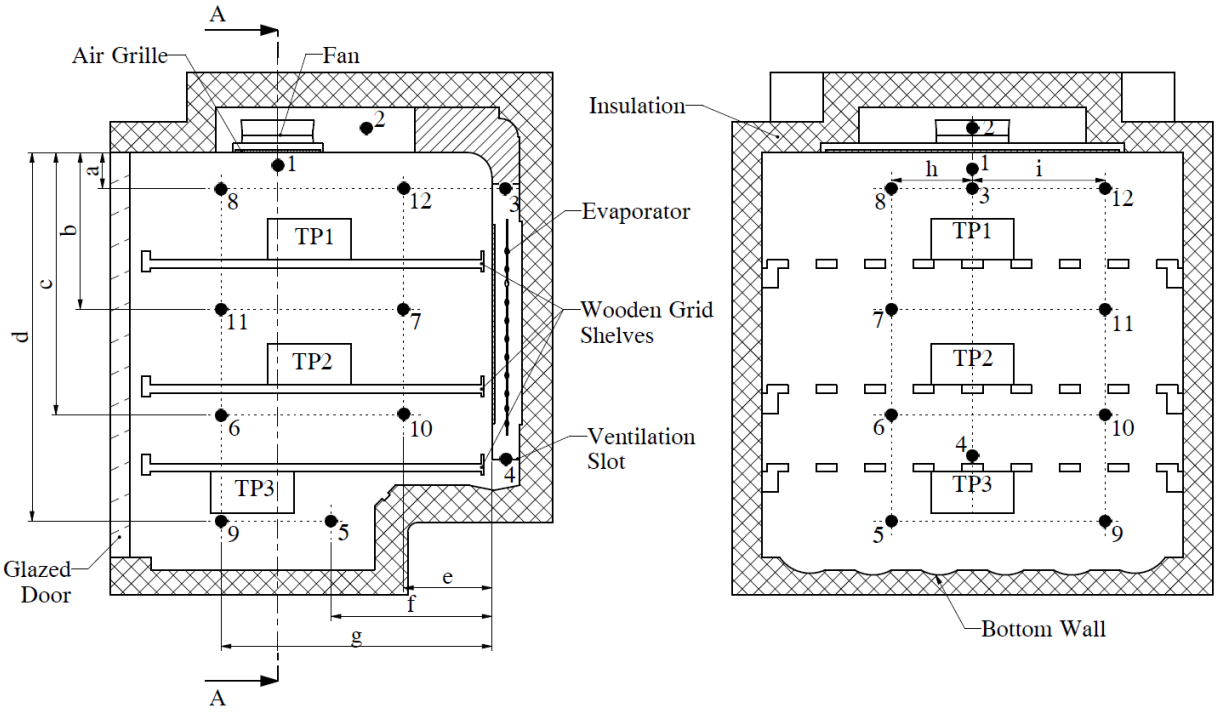

Figure 1: Distribution of the temperature measuring positions

Figure 2: Experimental setup – compartment, evaporator and close-up view of a measurement point

Table 1: Distances of the temperature measurement points

Distance	[mm]	Distance	[mm]
a	60	f	190
b	200	g	330
c	330	h	85
d	440	i	170
e	100		

3. SIMULATION MODEL

The computational domain can be divided into three different sections: the compartment, the air duct and the insulation. For the compartment two different configurations are investigated: empty – only with wooden grid shelves – and loaded with test packages. The section of the air duct reaches from the air grille across the fan and the evaporator up to the ventilation slot at the backside of the refrigerator. A cross section of the whole domain for the arrangement loaded with the test packages can be seen in Figure 1.

Due to the very complex geometry of the air duct, some simplifications have to be made to reduce the total number of cells. Firstly, the air grille, consisting of many small openings, is approximated by a porous media. Secondly, the fan is simplified by a pressure jump and last, the solid parts of the air duct such as walls or guiding plates are not modelled three-dimensionally. For the determination of the porous media parameters, a comparison between steady-state CFD simulations using the exact geometry of the air grille on the one side and the porous media on the other side is conducted. The parameters are adapted in order to result in similar pressure drops. The fan, used in the investigated wine storage cabinet, is continuously running but changes its rotational frequency depending on the ON- and OFF-period of the compressor. The frequency of the fan is 30 Hz and 18.7 Hz, respectively. Therefore, two different polynomial pressure jump – velocity functions are used to describe the pressure jump due to the fan. A tetrahedral mesh with 7.8 million cells is used, whereat 2.7 million cells are used in the section of the air duct, 3.9 million cells in the section of the compartment and the remaining cells for solid parts. The simulation takes 24 hours for one cycle (~50 minutes) consisting of one ON- and OFF period of the compressor (Dual CPU 8 Core 2.4GHz).

3.1 Main assumptions and boundary conditions

The numerical simulations are carried out using the finite volume CFD software ANSYS® Fluent 15. Assuming that variations in temperature only lead to small changes of the flow field, the energy equation and the flow field are solved separately. Based on the steady-state flow field, only the energy equation is solved transiently for 30 seconds. Afterwards the continuity and the momentum equations are solved for steady-state conditions again and the transient temperature field is calculated for another 30 seconds. The procedure of the solution process is shown in Figure 3.

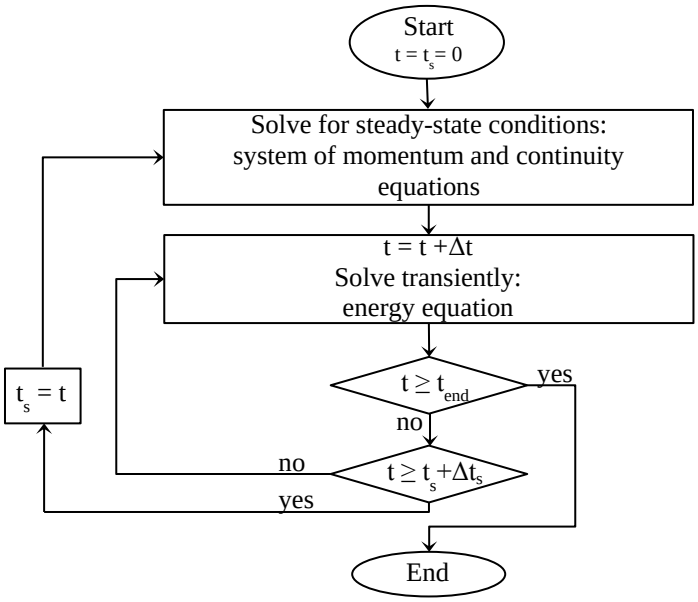

Figure 3: Procedure of the computational algorithm

Moreover, the following assumptions are made for the numerical analysis:

- Uniform temperature of the evaporator's surface (area weighted average based on experiments)
- Constant convective heat transfer coefficients (outside) and constant ambient temperature
- No radiation
- Incompressible flow due to a low Mach number
- No air leakage
- Turbulent flow conditions

The time-varying temperature boundary condition for the freely suspended evaporator is based on measurements. Therefore, the temperatures of three points distributed on the evaporator are measured over a period of several cycles and mean values based on an area weighted average are calculated. The cyclical temperature profile is then divided into three sections (I, II, III) which are approximated by polynomial functions. The measured and the approximated temperature profile over one cycle can be seen in Figure 4.

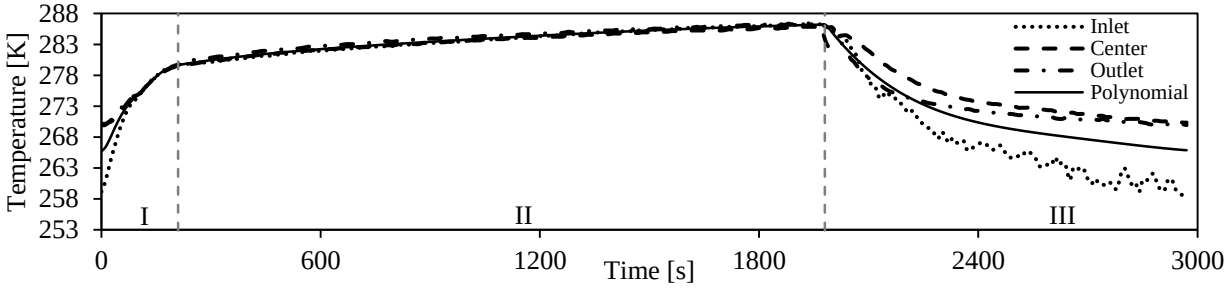

Figure 4: Transient temperature profile of the evaporator

A heat source considers the waste heat of the fan, which is 0.73 W during the ON-period of the compressor and 0.325 W otherwise. For all external walls with the exception of the bottom of the compartment, the ambient temperature T_{amb} is 24.5 °C and the convective heat transfer coefficient α is 5 W/m^{2}K. For the bottom wall, the values are 29 °C and 10 W/m^{2}K respectively, due to the heat release of the compressor and the condenser being located directly below. The properties of the solids used in this simulation can be seen in Table 2. Thereby, the material properties of glass refer to the averaged values of a double-glazed door.

Table 2: Physical properties of the solids

Solid	**ρ [kg/m³]**	**c_p [J/kg K]**	**λ [W/m K]**
Plastic	1050	1500	0.17
Insulation	50	1400	0.022
Glass (double-glazed)	834	840	0.08
Wood	700	2310	0.173
Test package	1000	3250	0.52

3.2 Mathematical model

Assuming an incompressible gas, the conservation equations of continuity, momentum and energy by neglecting viscous dissipation can be written in vector form as:

$$\vec{\nabla} \cdot \vec{u} = \vec{0} \tag{1}$$

$$\frac{d\vec{u}}{dt} = -\frac{1}{\varrho}\vec{\nabla}p + \nu\Delta\vec{u} + \vec{g}\frac{\beta(T - T_0)}{\varrho} \tag{2}$$

$$\frac{dT}{dt} = a\Delta T + \frac{\dot{q}_Q}{\rho\, c_p} \tag{3}$$

Thereby, the terms d*/dt are the substantial derivatives.

3.3 CFD methodology

The numerical simulations are carried out applying the commercial software ANSYS® Fluent. The two-equation turbulence model "realizable k-ε" is used with k and ε values of 1 and 1.2, respectively. The pressure based coupled solver algorithm is applied, which solves the momentum and pressure-based continuity equation simultaneously and the energy equation separately. Due to the use of a porous media and the "fan"-boundary condition, the Pressure Staggering Option (PRESTO) scheme is selected. For the transient calculation of the energy equation, a time step size Δt of 0.5 seconds is chosen and the convergence criterion is 1e-7. The steady-state calculations of the flow field are carried out for maximum 150 iterations for every specific time step (Δt_s=30 seconds) using a convergence criterion of 1e-3 for velocity components, continuity and turbulence model.

4. RESULTS

A time dependent analysis of the air flow and temperature stratification was conducted and temperatures at several positions inside the air duct and the compartment were compared with measurements. This analysis was carried out for the empty compartment, in which only wooden grid shelves are inside the refrigerator, and the compartment filled with three test packages. A fine tuning of the physical properties of the solid parts was done for the compartment filled with packages and the same properties were used for the simulation of the empty compartment.
Figure 5 shows temperature profiles of three different measurement points for the empty compartment (a, c and e) and the compartment loaded with test packages (b, d and f). The minimum and maximum temperature values of the simulation are mostly in acceptable accordance with the measuring data (thin dotted line). Nevertheless, deviations occur especially during the warming-up and cooling phase. This behavior can be explained by the usage of an averaged temperature boundary condition for the evaporator, neglecting the thermal mass of thermocouples and the strongly simplified walls, which results in an inexact consideration of the thermal masses. During the warm-up phase it also can be seen, that the influence of buoyancy forces is stronger due to the lower velocities which leads to a small oscillation of the simulated temperature profiles in the simulation. Conspicuously is the high temperature drop at the end of the cooling phase which results from the abrupt reduction of the fan speed and thus of reduced flow velocities.

A comparison between measured and simulated temperatures of all measurement points can be seen in Table 3 and Table 4, respectively. Therein, the minimum and maximum temperatures as well as the temperature differences (T_{max} - T_{min}) are given. These values are averaged temperatures to disregard influences of the noise in the measuring signals. Differences in temperature are mostly within 0.6 K. A detailed analysis of the simulations reveals that an inexact positioning of the thermocouple in regions with a high temperature gradient can also have an influence on the measurements which could explain the rather big deviation of measurement point 8. Furthermore, influences of the measuring instrumentation (cable, copper plate) on the air flow and the inaccurate positioning of it, cannot be excluded completely. Generally, simulations show that it is an important but very extensive task to find suitable boundary conditions. Especially the temperature profiles of the evaporator and the thermal mass of the solid parts can have big influences on the results.

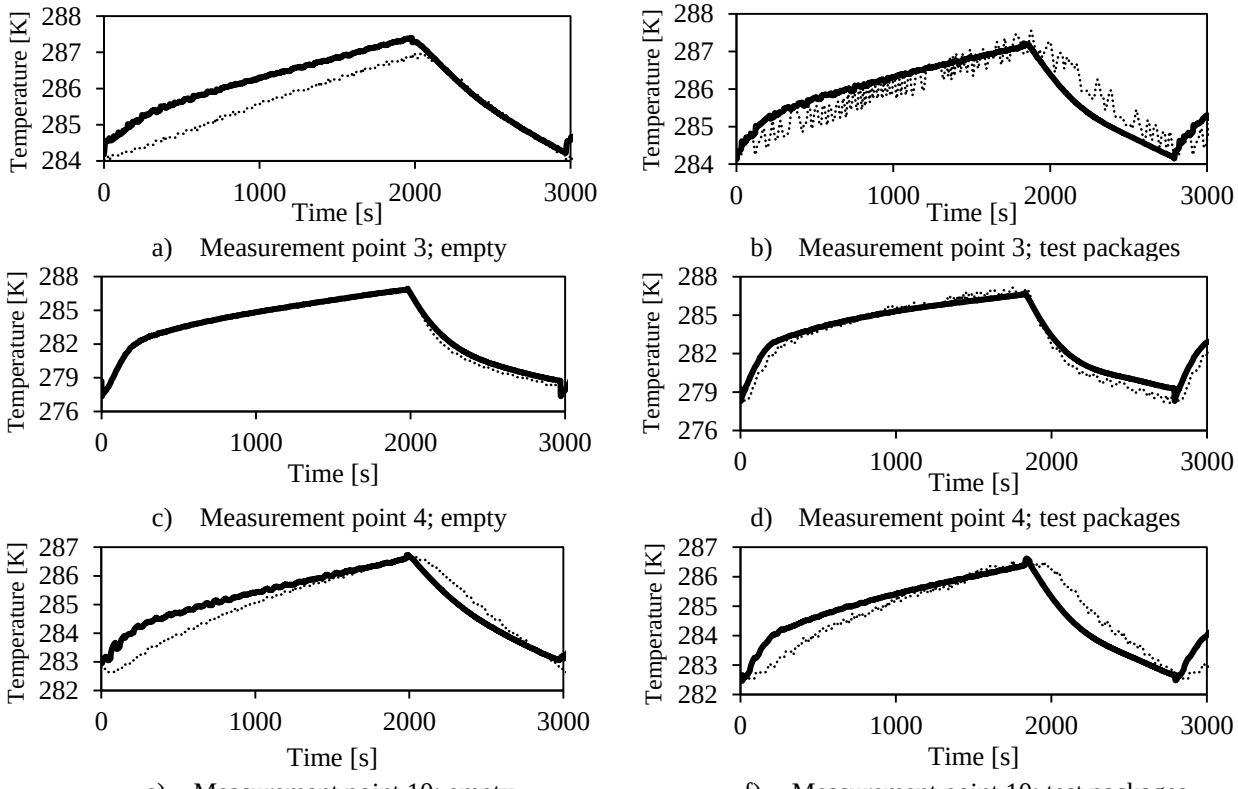

Figure 5: Temperature profiles during one cycle

Table 3: Comparison of temperature values between measurement and simulation – empty

	Measurement			Simulation		
Measurement Point	**ΔT [K]**	**T_{max} [K]**	**T_{min} [K]**	**ΔT [K]**	**T_{max} [K]**	**T_{min} [K]**
1	3.5	286.8	283.3	3.9	286.8	282.9
2	2.7	286.8	284.1	3.5	287.4	283.9
3	2.8	286.9	284.1	3.2	287.4	284.2
4	8.4	286.6	278.2	8.1	286.8	278.7
5	4.0	287.1	283.1	4.6	287.6	283.0
6	4.3	286.8	282.5	4.4	286.6	282.2
7	3.0	286.7	283.1	3.7	286.6	282.9
8	2.8	287.4	284.6	3.5	287.2	283.7
9	4.6	286.7	282.1	5.5	287.5	282.0
10	3.9	286.6	282.7	3.6	286.6	283.0
11	3.5	286.7	283.2	4.1	286.6	282.5
12	2.8	286.8	284.0	3.0	287.2	284.2

Table 4: Comparison of temperature values between measurement and simulation – test packages

	Measurement			Simulation		
Measurement Point	**ΔT [K]**	**T_{max} [K]**	**T_{min} [K]**	**ΔT [K]**	**T_{max} [K]**	**T_{min} [K]**
1	3.1	287.0	283.9	3.2	286.5	283.3
2	2.9	287.4	284.5	3.0	287.1	284.1
3	2.7	287.2	284.5	3.0	287.2	284.2
4	8.3	286.8	278.5	7.3	286.6	279.3
5	3.9	287.1	283.2	4.6	287.2	282.6
6	4.2	286.8	282.6	4.1	286.2	282.1
7	3.6	286.6	283.0	3.5	286.3	282.8
8	2.9	287.6	284.7	3.4	286.7	283.3
9	4.5	286.8	282.3	5.1	287.4	282.3
10	3.8	286.4	282.6	3.8	286.4	282.6
11	3.6	287.1	283.5	3.8	286.4	282.6
12	2.9	287.0	284.1	2.9	286.7	283.8
TP1	0.1	284.70	284.60	0.25	284.97	284.72
TP2	0.1	285.05	284.95	0.09	284.51	284.42
TP3	0.1	285.15	285.05	0.13	284.82	284.69

4.1 Empty Compartment

Figure 6a shows the air flow by means of streamlines inside the air duct and the compartment without loading. Air is sucked through the air grille by the axial fan and is blown against the top wall of the air duct, where the maximum velocities occur. Afterwards, the flow is evenly distributed along the entire width of the air duct by the guiding plates and streams over the freely suspended evaporator. Then, the air is blown inside the compartment through the ventilation slot and hits the drainage channel for condensation water, where it is diverted. From there, the main part of the cooled air is blown directly between the rods of the lower grid shelf towards the glazed door where it streams upwards to the inlet of the air grille. Smaller vortexes occur at the bottom of the compartment below the lowest grid shelf and along the rear wall of the compartment.

Figure 7 shows temperature fields of the compartment and the air duct in XY, YZ and ZX planes at different positions. It can be observed that the temperature distribution is not completely symmetrical which can be mainly explained by the asymmetric drainage channel for condensation water at the backside of the compartment. Higher temperature regions can be observed primarily at the bottom below the lowest grid shelf. The reasons are the very low air flow and the released heat of the condenser and the compressor which are located in the plinth below the compartment. Further regions at higher temperatures occur along the glazed door and in the front area of the compartment ceiling which is due to the higher heat transfer through the glazed door.

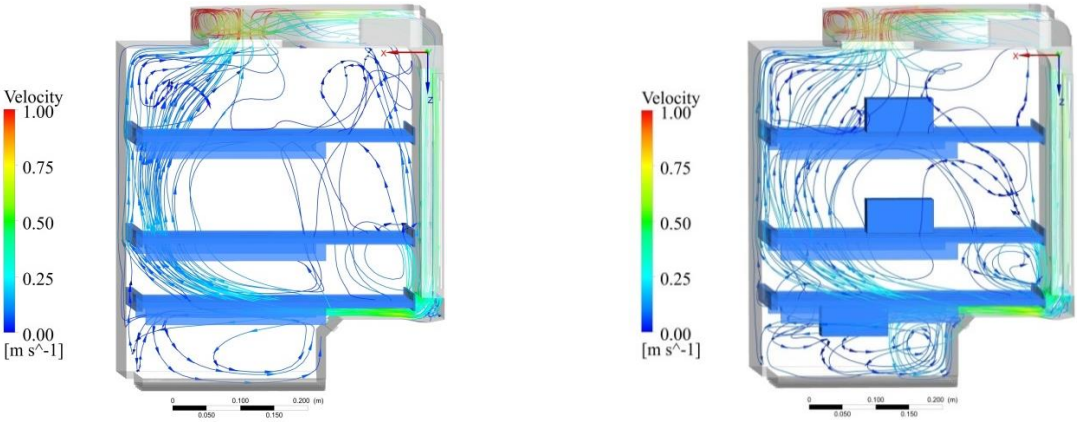

a) Empty compartment b) Compartment loaded with test packages

Figure 6: Air flow inside compartment and air duct

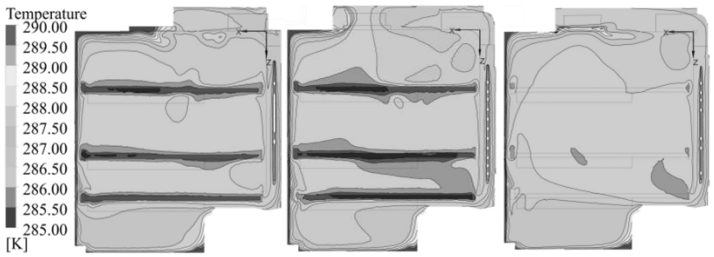

ZX-plane at Y = -170 mm, Y = 0 mm, Y = 85 mm

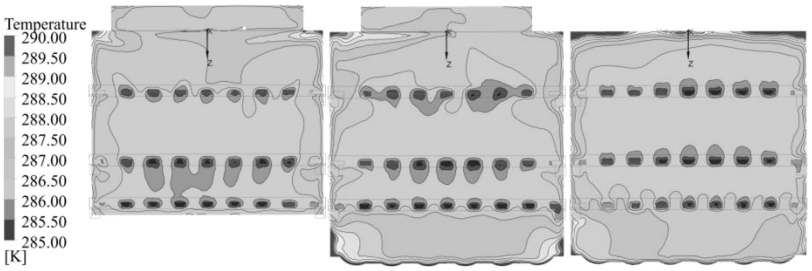

YZ-plane at X = 100 mm, X = 190 mm, X = 330 mm

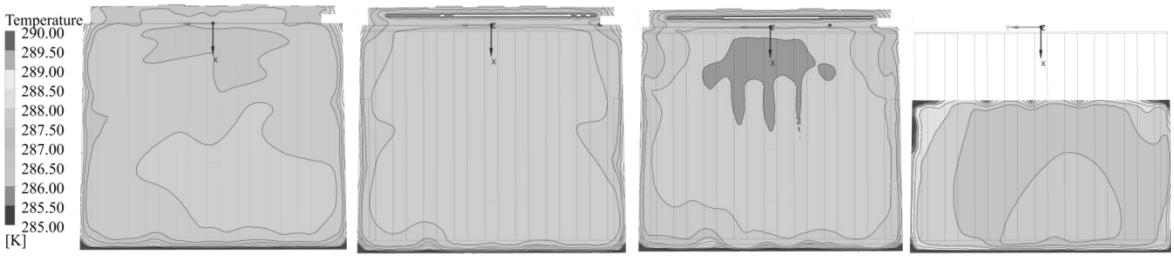

XY-plane at Z = 60 mm, Z = 200 mm, Z = 330 mm, Z = 440 mm

Figure 7: Temperature fields, arrangement empty, t = 1670 s

4.2 Compartment filled with test packages

Figure 6b shows the flow of the air by means of streamlines for the arrangement with test packages. Starting from the ventilation slot, three main flow directions can be observed. A large part of the cold air is blown directly between the rods of the lower wooden grid shelf above the lower test package. Then, the air streams along the door upwards to the inlet of the air grille. Another part of the cold air hits the lower package and is deflected downwards which leads to a vortex. The third part flows along the rear wall of the compartment towards the inlet of the air duct.

Figure 8 shows temperature fields of the compartment and the air duct in XY, YZ and ZX planes at different positions. Higher temperature regions can be observed at the bottom below the lower test package, along the door and in the front area of the compartment ceiling. Reasons for higher temperatures in the first mentioned area are the relatively weak current of air and the released heat of the compressor and the condenser. The higher heat transfer through the glazed door warms up the passing air which leads to the other two mentioned regions of higher temperature.

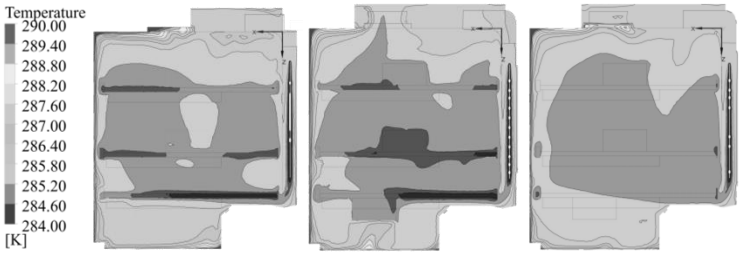

ZX-plane at Y = -170 mm, Y = 0 mm, Y = 85 mm

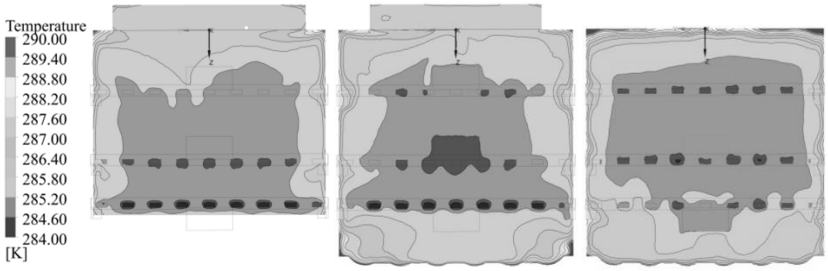

YZ-plane at X = 100 mm, X = 190 mm, X = 330 mm

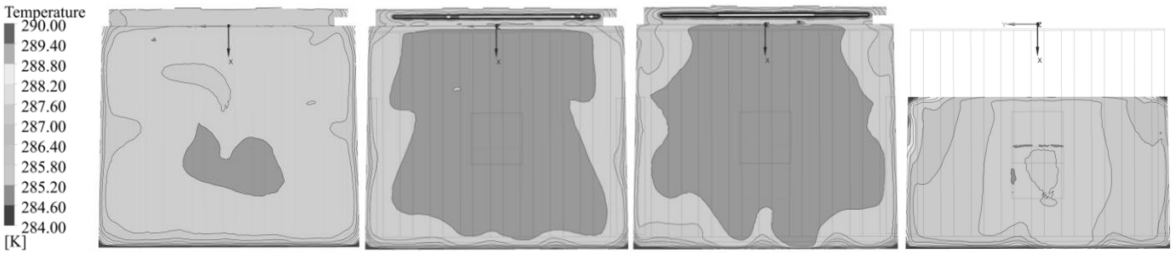

XY-plane at Z = 60 mm, Z = 200 mm, Z = 330 mm, Z = 440 mm

Figure 8: Temperature fields, arrangement with test packages, t = 1690 s

5. CONCLUSIONS

This work deals with the investigation of the temperature stratification and air flow inside the compartment of a wine storage cabinet. Experiments and CFD-simulations were done for two different configurations of the compartment: empty compartment only with wooden grid shelves and compartment loaded with test packages. The main focus of attention was the temperature evolution over a whole working cycle. The duration of one cycle is about 3000 seconds and would lead to an extremely long computational time if conventional solution approaches would be used. To reduce the computational effort, this paper uses an approach where the energy equation and flow field is solved in a decoupled way. This means, that the flow field is calculated at specific points in time assuming steady-state conditions and only the energy equation is solved transiently. The computational time for one cycle was approximately 24 hours. A comparison between measurements and simulation data shows that minimum and maximum values and therefore, the temperature spread could be calculated in a satisfying manner with the used approach. The situation is slightly different concerning the exact shape of the temperature profile. During the beginning of the ON- and OFF-period of the compressor, the simulations show a larger temperature gradient compared to the measurements. Simulations with slightly different boundary conditions indicate that:

- The influence of different profiles of the evaporator temperature on all other measurement points is much more significant than different air mass flow rates.

- An inexact approximation of the geometry can also lead to discrepancies between simulations and measurements due to a complex flow field.
- Another important influence factor is the adjustment of the thermal mass of solid parts.

In summary, it can be pointed out that the presented approach can be used to simulate the temperature evolution inside a refrigerator in a satisfying manner but with a much lower computational effort. To get more precise results, geometry and especially solid parts should be modelled more accurately.

NOMENCLATURE

a	thermal diffusivity	(m^2/s)
c_p	specific heat capacity	(J/kg K)
p	pressure	(Pa)
$\dot{q}_Q$	heat source	(W/m^3)
t	time	(s)
T	temperature	(K)
u	velocity	(m/s)

Greek Symbols

α	convective heat transfer coefficient	(W/m^2 K)
β	volumetric thermal expansion coefficient	(1/K)
λ	thermal conductivity	(W/m K)
ν	kinematic viscosity	(m^2/s)
ρ	density	(kg/m^3)

Subscripts

0	reference value
amb	ambient
s	steady-state

REFERENCES

Bayer, O., Ruknettin, O., Paksoy, A., Aradag, S. (2013). CFD simulations and reduced order modelling of a refrigerator compartment including radiation effects, *Energy Conversion and Management, 69*, 68-76.

Belman-Flores, J. M., Gallegos-Munoz, A., Puente-Delgado, A. (2014). Analysis of the temperature stratification of a no-frost domestic refrigerator with bottom mount configuration, *Applied Thermal Engineering, 65*(1-2), 299-307.

Ben Amara, S., Laguerre, O., Charrier-Mojtabi, M.-C., Lartigue, B., Flick, D. (2008). PIV measurement of the flow field in a domestic refrigerator model: Comparison with 3D simulations, *International Journal of Refrigeration, 31*(8), 1328-1340.

Bosseboeuf, D. (2015, June). Energy Efficiency Trends and Policies in the Household and Tertiary Sectors. Retrieved from http://www.odyssee-mure.eu/publications/br/

De Almeida, A., Fonseca, P., Schlomann, B., Feilberg, N. (2011). Characterization of the household electricity consumption in the EU, potential energy savings and specific policy recommendations, *Energy and Buildings, 43*(8), 1884-1894.

Fukuyo, K., Tanaami, T., Ashida, H. (2003). Thermal uniformity and rapid cooling inside refrigerators, *International Journal of Refrigeration, 26*(2), 249-255.

Hermes, C. J. L., Marques, M. E., Melo, C., Negrao, C. O. R. (2002). A CFD Model For Bouyancy Driven Flows Inside Refrigerated Cabinets and Freezers, *International Refrigeration and Air Conditioning Conference at Purdue*, West Lafayette, USA, Paper 608.

Laguerre, O., Ben Amara, S., Moureh, J., Flick, D. (2007). Numerical simulation of air flow and heat transfer in domestic refrigerators, *Journal of Food Engineering, 81*(1), 144-156.

Lee, I. S., Baek, S. J., Chung, M. K., Rhee, D. I. (1999). A study of air flow characteristics in the refrigerator using PIV and computational simulation, *Journal of Flow Visualization and Image Processing, 6*(4), 333-342.

Yang, K.-S., Chang, W.-R., Chen, I.-Y., Wang, C.-C. (2010). An investigation of a top-mounted domestic refrigerator, *Energy Conversion and Management, 51*(7), 1422-1427.

ACKNOWLEDGEMENT

This work has been carried out within the framework of ECO-COOL, a research project initiated and funded by the FFG (Austrian Research Promotion Agency). Furthermore the authors particularly acknowledge the technical support by Secop Austria GmbH, formerly ACC Austria GmbH and Liebherr-Hausgeräte Lienz GmbH.